Thermoelectric Polarization Transport in Ferroelectric Ballistic Point Contacts

Ping Tang,[1] Ryo Iguchi,[2] Ken-ichi Uchida,[2,3,4] and Gerrit E. W. Bauer[1,3,4,5]
[1]WPI-AIMR, Tohoku University, 2-1-1 Katahira, 980-8577 Sendai, Japan
[2]National Institute for Materials Science, Tsukuba 305-0047, Japan
[3]Institute for Materials Research, Tohoku University, 2-1-1 Katahira, 980-8577 Sendai, Japan
[4]Center for Spintronics Research Network, Tohoku University, Sendai 980-8577, Japan
[5]Zernike Institute for Advanced Materials, University of Groningen, 9747 AG Groningen, Netherlands

(Received 1 June 2021; accepted 30 November 2021; published 25 January 2022)

We formulate a scattering theory of polarization and heat transport through a ballistic ferroelectric point contact. We predict a polarization current under either an electric field or a temperature difference that depends strongly on the direction of the ferroelectric order and can be detected by its magnetic stray field and associated thermovoltage and Peltier effect.

DOI: 10.1103/PhysRevLett.128.047601

Orifices such as Maxwell-Sharvin point contacts [1,2], microstructured and nanostructured constrictions such as semiconductor quantum point contacts [3,4] and atomic-scale break junctions [5], etc., are important instruments to study transport properties in condensed matter physics on small length scales. The quantization of transport of electrons [6,7], light [8], super- [9,10], and spin [11,12] currents as well as photonic [13,14], electronic [15–17], and phononic [18–20] heat currents are some of the important breakthroughs in this field. To the best of our knowledge, the transport through constrictions formed by *ferroelectrics* has never been addressed, neither theoretically nor experimentally.

Ferroelectricity refers to the electrically switchable macroscopic order of electric dipoles or persistent polarization that forms spontaneously below a Curie temperature [21] with some analogies with magnetism [22]. In so-called displacive ferroelectrics, the phase transition is accompanied by a symmetry-breaking structural phase transition: ferroelectricity is then caused by short-range elastic forces, while magnetism is caused by the short-range exchange interaction. The dipolar interaction is much larger in ferroelectrics than in ferromagnets and causes important secondary effects.

The elementary excitations of the magnetic order, i.e., spin waves or magnons, can transport energy, linear, and spin angular momentum. In high-quality magnetic insulators, coherently excited magnons with long wavelengths travel ballistically over large distances [23]. Thermal magnons, on the other hand, propagate diffusely under a gradient of temperature, magnetic field, or chemical potential [24], causing the spin Seebeck [25] and Peltier effects [26,27]. Here, we address the question of whether analogous transport processes exist in ferroelectrics. Previously we proposed diffuse polarization transport in ferroelectric capacitors [28].

In this Letter, we formulate ballistic transport through constrictions of a displacive ferroelectric by the scattering theory of transport [19,29,30]. In contrast to the findings for diffuse systems [28], we predict a polarization current that generates observable stray magnetic fields as well as a dc polarization Peltier effect within the relaxation time of the reservoirs. Hereafter, "dc" refers to the transport regime within this timescale [31].

We consider a monolithic ferroelectric sample in which a narrow wire adiabatically connects two reservoirs with perpendicular ferroelectric order at temperatures sufficiently below the phase transition. The two reservoirs are at thermal equilibrium but at possibly different temperature T_1 and T_2. Top and bottom gates allow application of different electric fields E_1 and E_2 as sketched in Fig. 1(a).

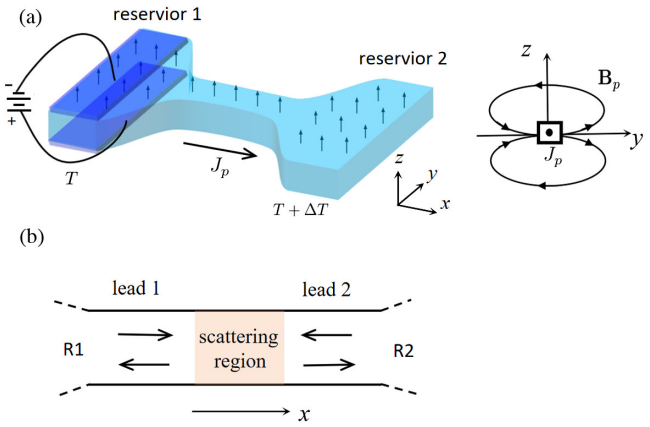

FIG. 1. (a) Polarization transport between two ferroelectric reservoirs ($R1$ and $R2$) connected by a ferroelectric lead (left panel). The polarization current induces a magnetic field (right panel). In accordance with the polarization current direction as in (a), there are an electric field applied on the $R1$ along the direction of ferroelectric order and a temperature difference ($\Delta T > 0$) on the $R2$. (b) The ferroelectric lead is divided by the scattering region into two parts of lead 1 and 2 that are in adiabatic contact with the $R1$ and $R2$, respectively.

We focus on steady-state transport, which requires sufficiently large reservoirs. In linear response, currents and forces are related by a matrix of transport coefficients [28]

$$\begin{pmatrix} -J_p \\ J_q \end{pmatrix} = G \begin{pmatrix} 1 & S \\ \Pi & K/G \end{pmatrix} \begin{pmatrix} \Delta E \\ -\Delta T \end{pmatrix}, \tag{1}$$

where the J_p and J_q are the polarization and heat currents flowing from reservoir 1 to 2, while $\Delta E = E_2 - E_1$ and $\Delta T = T_2 - T_1$ are the electric field and temperature differences between the two reservoirs, respectively. G is the polarization conductance, S (Π) the polarization Seebeck (Peltier) coefficient with Kelvin-Onsager relation $\Pi = ST$, and K the thermal conductance. We now derive all transport coefficients by the scattering theory of transport.

Phonon model.—A phonon mode in a wire along the x axis with wave number k reads

$$\boldsymbol{u}_{nk\sigma}(l,s) = \frac{1}{\sqrt{NM_s}} \mathbf{e}_{nk\sigma}(s) \varphi_n(\boldsymbol{\rho}_l) e^{ikx_l - i\omega_{nk\sigma}\tau}, \tag{2}$$

where $\boldsymbol{u}_{nk\sigma}(l,s)$ is the displacement of the s-th ion in the l-th ferroelectric unit cell, with the ionic mass of M_s, N the number of unit cells. Here, $\omega_{nk\sigma}$ is the phonon frequency dispersion, $\mathbf{e}_{nk\sigma}(s)$ the polarization vector of phonon with polarization index $\sigma = 1, \ldots, 3m$, where m is the number of ions in each ferroelectric unit cell, with band index n and $\boldsymbol{\rho}_l$ the transverse coordinate. The orthogonality relations are $\sum_l \varphi_n(\boldsymbol{\rho}_l)\varphi_{n'}(\boldsymbol{\rho}_l)^* e^{i(k-k')x_l} = N\delta_{nn'}\delta_{kk'}$ and $\sum_s \mathbf{e}_{nk\sigma}(s) \cdot [\mathbf{e}_{nk\sigma'}(s)]^* = \delta_{\sigma\sigma'}$.

A phonon $\boldsymbol{u}_{nk\sigma}$ originating in the left reservoir ($R1$) with positive group velocity $v_{nk\sigma} = \partial\omega_{nk\sigma}/\partial k > 0$ can be elastically reflected or transmitted by the constriction, as illustrated in Fig. 1(b), and the amplitude in both leads then reads

$$\boldsymbol{u}^{(1)}_{nk\sigma} = \begin{cases} \boldsymbol{u}_{nk\sigma} + \sum_{n',\sigma'} \boldsymbol{u}_{n'-k'\sigma'} r_{n'\sigma'n\sigma} & \text{in lead 1,} \\ \sum_{n',\sigma'} \boldsymbol{u}_{n'k'\sigma'} t_{n'\sigma'n\sigma} & \text{in lead 2,} \end{cases} \tag{3}$$

where $r_{n'\sigma'n\sigma}$ is the reflection amplitude from mode $n\sigma$ to $n'\sigma'$ in lead 1, while $t_{n'\sigma'n\sigma}$ is the transmission amplitude from mode $n\sigma$ in lead 1 to $n'\sigma'$ in lead 2 and $\omega_{nk\sigma} = \omega_{n'k'\sigma'}$ for the elastic scattering. Analogously, assuming that the junction is symmetric, an incoming phonon $\boldsymbol{u}_{nk\sigma}$ from the right reservoir ($R2$) generates the following amplitudes in both leads

$$\boldsymbol{u}^{(2)}_{n-k\sigma} = \begin{cases} \sum_{n',\sigma'} \boldsymbol{u}_{n'-k'\sigma'} t_{n'\sigma'n\sigma} & \text{in lead 1,} \\ \boldsymbol{u}_{n-k\sigma} + \sum_{n',\sigma'} \boldsymbol{u}_{n'k'\sigma'} r_{n'\sigma'n\sigma} & \text{in lead 2.} \end{cases} \tag{4}$$

The total displacement field operator in the leads can then be written as [19]

$$\hat{\boldsymbol{u}}(l,s) = \sum_{n,\sigma,k>0} \sqrt{\frac{\hbar}{2\omega_{nk\sigma}}} [\hat{a}^{(1)}_{nk\sigma} \boldsymbol{u}^{(1)}_{nk\sigma}(l,s) + \hat{a}^{(2)}_{n-k\sigma} \boldsymbol{u}^{(2)}_{n-k\sigma}(l,s)] + \text{H.c.}, \tag{5}$$

where $\hat{a}^{(1)}_{nk\sigma}$ ($\hat{a}^{(2)}_{n-k\sigma}$) represents the creation operator of phonons originating in $R1$ ($R2$) and H.c. denotes the Hermitian conjugate of the previous term.

We adopt the standard rigid-ion approximation for displacive ferroelectrics [32,33] with polarization fluctuations around the ground state,

$$\Delta\hat{\mathbf{P}}_l = \sum_s Q_s \hat{\boldsymbol{u}}(l,s), \tag{6}$$

where Q_s is the ionic charge of the s-th ion in the ferroelectric unit cell with index l and $\sum_s Q_s = 0$. The polarization projection along the ferroelectric order in the l-th unit cell $\hat{P}_l = (P_0 + \Delta\hat{P}^{\parallel}_l)\cos\Delta\hat{\theta}_l$, where $\Delta\hat{P}^{\parallel}_l$ is the oscillation of the polarization modulus relative to $P_0 = |\mathbf{P}_0|$ in the ground state and $\Delta\hat{\theta}_l$ a small angle of rotation. We now make the *ferron* approximation that the fluctuations in $\Delta\hat{P}^{\parallel}_l$ and $\Delta\hat{\theta}_l$ are uncorrelated, which is justified when the longitudinal elastic constant of the dipole is sufficiently larger than the transverse one and excellent for the order-disorder type of ferroelectrics with stable molecular dipoles [34]. To leading order in small *Cartesian* transverse and longitudinal fluctuations, i.e., $\Delta\hat{\mathbf{P}}^{\perp}_l = \Delta\hat{\mathbf{P}}_l - (\Delta\hat{P}_l \cdot \mathbf{P}_0)\mathbf{P}_0/P_0^2$ and $\Delta\hat{P}^{\parallel}_l = \Delta\hat{\mathbf{P}}_l \cdot \mathbf{P}_0/P_0$,

$$\hat{P}_l = P_0 \left[1 - \frac{(\Delta\hat{\mathbf{P}}^{\perp}_l)^2}{2P_0^2}\right] + \Delta\hat{P}^{\parallel}_l + \mathcal{O}[(\Delta\hat{\mathbf{P}}^{\perp}_l)^2, \Delta\hat{P}^{\parallel}_l]. \tag{7}$$

The first term captures the reduced polarization projection along the ferroelectric order by the transverse fluctuations and we disregard $\Delta\hat{P}^{\parallel}_l$ and higher-order terms.

When the polarization is conserved on the length scale of the constriction, the operator for the coarse-grained polarization density $\hat{P}_l/\Omega \to \hat{p}(\mathbf{r},\tau)$ per unit cell with volume Ω is related to the polarization current density $\hat{\jmath}_p(\mathbf{r},\tau)$ through

$$\partial_x \hat{\jmath}_p(\mathbf{r},\tau) = -\partial_\tau \hat{p}(\mathbf{r},\tau), \tag{8}$$

where $\mathbf{r} \equiv (x,\boldsymbol{\rho})$ and the operators are in the Heisenberg picture. The partial Fourier transform $\hat{p}(\boldsymbol{\rho},q,\omega) = \int d\tau \int dx \hat{p}(\boldsymbol{\rho},x,\tau) e^{i\omega\tau - iqx}$ leads to

$$\hat{\jmath}_p(\mathbf{r},\tau) = \int \frac{dq}{2\pi} \int \frac{d\omega}{2\pi} \left(\frac{\omega}{q}\right) \hat{p}(\boldsymbol{\rho},q,\omega) e^{-i\omega\tau + iqx}. \tag{9}$$

Substituting Eq. (7) and to leading order in the fluctuations Eq. (6), the statistical average of the total polarization current

$$J_p \equiv \int d\boldsymbol{\rho}\langle \hat{j}_p(\mathbf{r},\tau)\rangle = -\frac{\hbar}{2P_0}\sum_{n',\sigma'}\sum_{n,\sigma}\int_0^{\mathrm{BZ}}\frac{dk}{2\pi}\frac{|\boldsymbol{F}^{\perp}_{n'k'\sigma'}|^2}{\omega_{n'k'\sigma'}} v_{n'k'\sigma'}|t_{n'\sigma'n\sigma}|^2 \times [\langle \hat{a}^{\dagger}_{nk\sigma}\hat{a}_{nk\sigma}\rangle^{(1)} - \langle \hat{a}^{\dagger}_{n-k\sigma}\hat{a}_{n-k\sigma}\rangle^{(2)}], \tag{10}$$

where BZ indicates the Brillouin zone boundary. Here $\boldsymbol{F}^{\perp}_{nk\sigma} = \boldsymbol{F}_{nk\sigma} - (\mathbf{F}_{nk\sigma}\cdot\mathbf{P}_0)\mathbf{P}_0/P_0^2$ is the transverse component of

$$\boldsymbol{F}_{nk\sigma} = \sum_s \frac{Q_s}{\sqrt{M_s}}\mathbf{e}_{nk\sigma}(s) \tag{11}$$

and $\langle\cdots\rangle^{(i)}$ is a thermal average in reservoir i:

$$\langle \hat{a}^{\dagger}_{nk\sigma}\hat{a}_{nk\sigma}\rangle^{(i)} = N(\hbar\omega_{nk\sigma} - \mu^{(i)}_{nk\sigma}, T^{(i)}). \tag{12}$$

The parameters in the Planck distribution function $N(\hbar\omega,T) \equiv 1/[e^{\hbar\omega/k_BT}-1]$ are the temperature $T^{(i)}$ and effective chemical potential $\mu^{(i)}_{nk\sigma} = \xi_{nk\sigma}E^{(i)}$, where $E^{(i)}$ is the electric field of reservoir i and polarization

$$\xi_{nk\sigma} = -\frac{\hbar}{2P_0}\frac{|\boldsymbol{F}^{\perp}_{nk\sigma}|^2}{\omega_{nk\sigma}}. \tag{13}$$

In the above calculations we adopted the conventional assumption of an adiabatic connection between the reservoirs and the leads. The electric fields are applied on the reservoirs where they affect the equilibrium phonon statistics. In linear response, transport is then only governed by the differences in $E^{(i)}$ and $T^{(i)}$ in the reservoirs and the transmission coefficients through the constriction. We consider here two different configurations, viz., with equilibrium polarization in the constriction normal to the plane (parallel to those in the reservoirs) and along the wire. They can in principle be switched by the electric fields of local gates, but we assume here for simplicity that the field in the constriction vanishes.

The energy or heat current reads

$$J_q = \sum_{n'\sigma'}\sum_{n\sigma}\int_0^{\mathrm{BZ}}\frac{dk}{2\pi}\hbar\omega_{n'k'\sigma'}v_{n'k'\sigma'}|t_{n'\sigma'n\sigma}|^2 \times [N(\hbar\omega_{nk\sigma}-\mu^{(1)}_{nk\sigma},T^{(1)}) - N(\hbar\omega_{nk\sigma}-\mu^{(2)}_{nk\sigma},T^{(2)})]. \tag{14}$$

In the ballistic limit, $t_{n'\sigma'n\sigma} = \delta_{nn'}\delta_{\sigma\sigma'}$

$$J_q = -\sum_{n\sigma}\int_{\omega^{\min}_{n\sigma}}^{\omega^{\max}_{n\sigma}}\frac{d\omega}{2\pi}\hbar\omega[N(\hbar\omega-\mu^{(2)}_{n\sigma}(\omega),T^{(2)}) - N(\hbar\omega-\mu^{(1)}_{n\sigma}(\omega),T^{(1)})], \tag{15}$$

where $\omega^{\min}_{n\sigma}$ and $\omega^{\max}_{n\sigma}$ are the band edges of the $n\sigma$ phonon mode, which in the absence of an electric field or ferroelectric order reduces to the conventional phonon heat current expression [18,19]. We obtain the transport coefficients in Eq. (1) by linearizing the distribution functions:

$$G = -\frac{1}{\hbar}\sum_{n\sigma}\int_{\omega^{\min}_{n\sigma}}^{\omega^{\max}_{n\sigma}}\xi^2_{n\sigma}(\omega)\left(\frac{\partial N}{\partial\omega}\right)_T\frac{d\omega}{2\pi},$$
$$\Pi = ST = G^{-1}\sum_{n\sigma}\int_{\omega^{\min}_{n\sigma}}^{\omega^{\max}_{n\sigma}}\omega\xi_{n\sigma}(\omega)\left(\frac{\partial N}{\partial\omega}\right)_T\frac{d\omega}{2\pi},$$
$$K = \sum_{n\sigma}\int_{\omega^{\min}_{n\sigma}}^{\omega^{\max}_{n\sigma}}\hbar\omega\left(\frac{\partial N}{\partial T}\right)_\omega\frac{d\omega}{2\pi}, \tag{16}$$

which (for simple ferroelectrics) are positive since $\partial N(\omega,T)/\partial\omega < 0$.

Diatomic ferroelectric chain.—For concreteness, we model transport properties at temperatures sufficiently below the ordering transition by a one-dimensional dimer chain, with two ions of opposite charges $\pm Q$ and same mass M in the unit cell, as sketched in Fig. 2 for the polarization perpendicular and parallel to the chain. The ground state permanent electric dipole in each unit cell is $P_0 = Q\delta$, where δ is the symmetry-breaking deformation and Q the ionic charge. For strongly anisotropic systems this model holds by multiplying the results with the number of parallel wires.

In the perpendicular configuration, only two optical phonons with polarization vector transverse to the ferroelectric order carry an average polarization of $\xi_{k\sigma} = -(\hbar Q^2)/(MP_0\omega_{k\sigma})$. Using the results from the Supplemental Material [35]

$$G = \frac{2\xi_P^2}{h}\int_{\sqrt{2}\epsilon_0}^{\sqrt{6}\epsilon_0}d\epsilon\frac{\epsilon_0^2e^{\epsilon}}{\epsilon^2(e^{\epsilon}-1)^2}, = \frac{\xi_P^2}{h}\begin{cases} e^{-\sqrt{2}\epsilon_0} - \frac{1}{3}e^{-\sqrt{6}\epsilon_0} & \text{for } k_BT \ll \hbar\omega_0, \\ \left(\frac{1}{3\sqrt{2}} - \frac{1}{9\sqrt{6}}\right)\frac{k_BT}{\hbar\omega_0} & \text{for } k_BT \gg \hbar\omega_0, \end{cases} \tag{17}$$

$$\Pi = \left(\frac{2\xi_P^2}{hG}\right)\frac{C\delta^2}{P_0}\int_{\sqrt{2}\epsilon_0}^{\sqrt{6}\epsilon_0}d\epsilon\frac{e^{\epsilon}}{(e^{\epsilon}-1)^2} = \frac{C\delta^2}{P_0}\begin{cases} 2 & \text{for } k_BT \ll \hbar\omega_0, \\ \frac{18}{13}(4-\sqrt{3}) & \text{for } k_BT \gg \hbar\omega_0, \end{cases} \tag{18}$$

$$K \approx \frac{k_B^2T}{h}\left[\int_0^{2\epsilon_0}d\epsilon\frac{3\epsilon^2e^{\epsilon}}{(e^{\epsilon}-1)^2} + \int_{\sqrt{2}\epsilon_0}^{\sqrt{6}\epsilon_0}d\epsilon\frac{2\epsilon^2e^{\epsilon}}{(e^{\epsilon}-1)^2}\right] = \begin{cases} \frac{\pi^2k_B^2T}{h} & \text{for } k_BT \ll \hbar\omega_0, \\ (3+\sqrt{6}-\sqrt{2})\frac{k_B\omega_0}{\pi} & \text{for } k_BT \gg \hbar\omega_0, \end{cases} \tag{19}$$

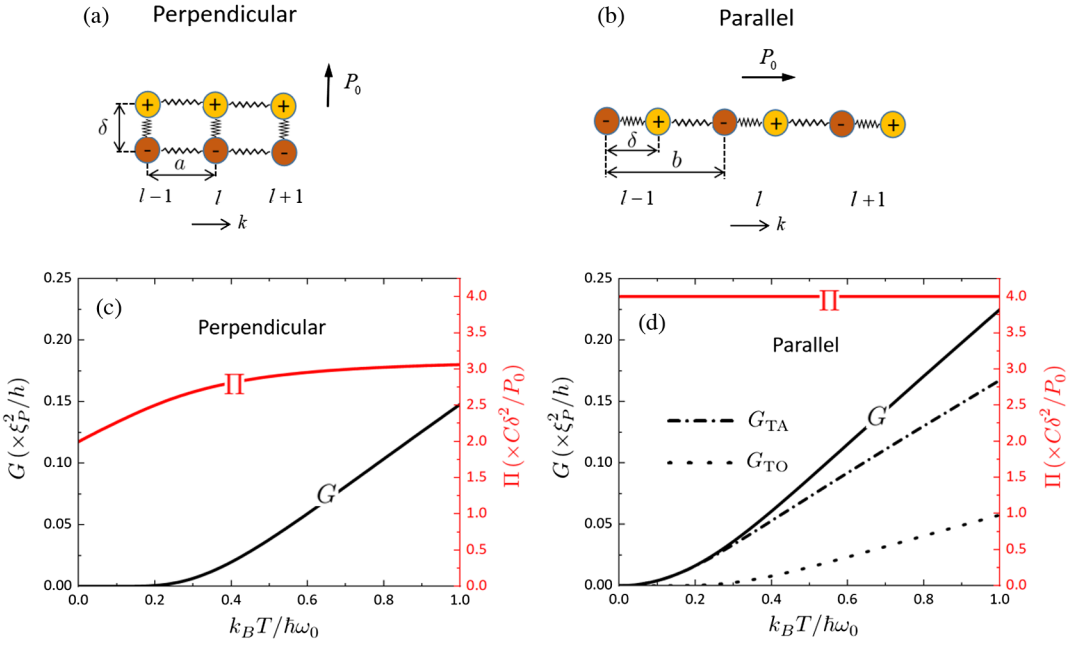

FIG. 2. Diatomic ferroelectric chains with spontaneous polarization (a) perpendicular and (b) parallel to the chain axis, respectively. The polarization conductance (G) and Peltier coefficient (Π) as a function of temperature for the perpendicular (c) and parallel (d) configurations, where TA and TO in (d) represent the contributions from the transverse acoustic and optical phonons, respectively.

where $\omega_0 = \sqrt{C/M}$ is the characteristic frequency of lattice vibration with C the shear force constant, $\xi_P = \hbar\omega_0 P_0/(C\delta^2)$ is a quantum polarization, analogous to the Bohr magneton for magnetization with $-\xi_P E/\hbar$ equivalent to the Rabi frequency, $\epsilon_0 = \hbar\omega_0/k_BT$ and $(0, 2\epsilon_0)$ and $(\sqrt{2}\epsilon_0, \sqrt{6}\omega_0)$ are the band edges in unit of k_BT for three acoustic and two transverse optical phonon modes, respectively [35]. The ratio between the elastic energy and electric dipole $C\delta^2/P_0$ also governs transport in the diffuse model [28]. In Fig. 2(c), we plot the polarization conductance and Peltier coefficient as a function of temperature (see Fig. S2 in Supplemental Material [35] for the heat conductance). Since the polarization transport is contributed by gapped optical phonons, G is exponentially small when $k_BT \ll \hbar\omega_0$. In contrast to $K = \pi^2 k_B^2 T/h$, the well-known quantum of phononic heat conductance [18–20], the polarization Peltier quantum $\Pi = C\delta^2/P_0$ is not universal, but depends on the material parameters.

Aligning the polarization with the wire axis drastically changes the polarization transport that is then carried by both transverse acoustic and optical phonon modes. According to the Supplemental Material [35]

$$\xi_{k\sigma} = -\frac{\hbar\omega_{k\sigma}P_0}{4C\delta^2}, \tag{20}$$

where $\sigma = \mathrm{TA}, \mathrm{TO}$ denotes the transverse acoustic and optical phonons, respectively, and Eq. (16) reduces to

$$K = \frac{k_B^2 T}{h}\int_0^{2\epsilon_0} d\epsilon \frac{3\epsilon^2 e^\epsilon}{(e^\epsilon - 1)^2} = \begin{cases} \frac{\pi^2 k_B^2 T}{h} & \text{for } k_BT \ll \hbar\omega_0, \\ \frac{3k_B\omega_0}{\pi} & k_BT \gg \hbar\omega_0, \end{cases} \tag{21}$$

$$G = \frac{\xi_P^2}{8h}\int_0^{2\epsilon_0} d\epsilon \frac{\epsilon^2 e^\epsilon}{\epsilon_0^2(e^\epsilon - 1)^2} = \frac{2}{3}\frac{KT}{\Pi^2}, \tag{22}$$

$$\Pi = \frac{4C\delta^2}{P_0}. \tag{23}$$

Here, Π is constant and the conductance G vanishes quadratically with temperature since polarization transport by the transverse acoustic phonons is massless at low energies. The figure of merit of thermal polarization transport turns out to be constant as well:

$$ZT \equiv \frac{G\Pi^2}{KT} = \frac{2}{3}. \tag{24}$$

Detection of polarization current.—In the steady state the polarization current from the high-field to the low field region is accompanied by a heat current. We assume in the derivations above that the reservoirs are such large that on the time scale of the transport process the bias is constant. Finite reservoirs react parametrically to these currents on a larger time scale. The Peltier effect can be observed by an increased temperature in the high-field regime and cooling of the low-field terminal, while the "battery" becomes depleted. When the two reservoirs are not electrically

biased but subject to a temperature difference, a heat current flows, accompanied by a Seebeck polarization current. Both currents contribute to an increase (decrease) of the polarization on the hot (cold) side that charges the capacitors by both pyroelectric and Seebeck effects, i.e., generates thermovoltages in both reservoirs. With the model parameters above we can compute the time dependence for given sample geometries parametrically.

The dc transport of electric polarization is accompanied by dc stray magnetic fields and, vice versa, an applied magnetic field can affect the polarization current. When flowing along the x with polarization along z as in Fig. 1(a), the magnetic flux density at a position $\mathbf{r} = (0, y, z)$ follows from the Lorentz transformation

$$\mathbf{B}_p = \frac{\mu_0 J_p}{2\pi\rho^2}(0, \cos 2\phi, \sin 2\phi), \tag{25}$$

where J_p is the polarization current, $\rho = \sqrt{y^2 + z^2}$ the probing distance, $\cos\phi = y/\rho$ and $\sin\phi = z/\rho$. For N_0 uncoupled parallel chains $J_p = N_0 G[\Delta E + \Pi(\Delta T/T)]$, where G and Π are the polarization conductance and Peltier coefficient for the single chain, respectively. In the perpendicular polarization configuration at $T = 300$ K, with $C = 25$ J/m^2, $\omega_0 = 10$ THz, $\delta = 0.03$ nm, $P_0 = 2 \times 10^{-29}$ Cm, which are close to those of conventional ferroelectrics of $BaTiO_3$ [36,37], we arrive at $G = 9.74 \times 10^{-28}$ m$^2/\Omega$, $\Pi = 3.52 \times 10^9$ V/m. The induced magnetic field for $N_0 = 1$ at a distance $\rho = 10$ nm is $B_p \approx 200$ pT for either $\Delta E = 10^8$ V/m or $\Delta T = 10$ K, which can be detected by single diamond-NV center magnetometry enhanced by spin-to-charge NV readout protocols [38]. The stray magnetic fields generated by the polarization current in thicker wires and tuned by the sample geometry may become large enough to be detectable by conventional sensors. References [39,40] predicted that circularly polarized optical phonons induce finite magnetic moments, which was subsequently confirmed [41]. The magnetic field generated by polarization current can be viewed as another form of multiferroicity.

Conclusions.—We derive expressions for the steady state polarization and heat transport through a ferroelectric constriction driven by temperature and electric field differences. We find drastic effects of rotating the polarization direction, such as an algebraic vs exponential suppression of the polarization current. The results can be extended to include, e.g., the effects of ferroelectric domain walls. The polarization current can be detected indirectly via the polarization Peltier effect and a thermovoltage or, more directly, by the stray magnetic field that accompanies the streaming dipoles. Our formulation for the polarization transport is not limited to this simple chain model but is accessible to first-principles calculations. The thermally and electrically induced transport of electric polarization opens alternative strategies for thermal management using ferroelectric materials. Our predictions require a persistent polarization which arises spontaneously in ferroelectrics, but may also be induced by, e.g., strong electric fields in paraelectric materials.

We acknowledge helpful discussions with Bart van Wees, Toeno van der Sar, Tomoya Nakatani, Toshu An, Kei Yamamoto, and Weichao Yu. P. T. and G. B. are supported by JSPS KAKENHI Grant No. 19H00645. R. I. and K. U. by JSPS KAKENHI Grant No. 20H02609, JST CREST "Creation of Innovative Core Technologies for Nano-enabled Thermal Management" Grant No. JPMJCR17I1, and the Canon Foundation.

[1] J. C. Maxwell, *A Treatise on Electricity and Magnetism* (Clarendon Press, Oxford, 1873), Vol. 1.
[2] Y. V. Sharvin, Zh. Eksp. Teor. Fiz. **48**, 984 (1965) [Sov. Phys. JETP **21**, 655 (1965)].
[3] H. van Houten, L. W. Molenkamp, C. W. J. Beenakker, and C. T. Foxon, Semicond. Sci. Technol. **7**, B215 (1992).
[4] H. van Houten and C. W. J. Beenakker, Phys. Today **49**, No. 7, 22 (1996).
[5] N. Agrait, A. L. Yeyati, and J. M. Van Ruitenbeek, Phys. Rep. **377**, 81 (2003).
[6] B. J. Van Wees, H. Van Houten, C. W. J. Beenakker, J. G. Williamson, L. P. Kouwenhoven, D. Van der Marel, and C. T. Foxon, Phys. Rev. Lett. **60**, 848 (1988).
[7] D. A. Wharam, T. J. Thornton, R. Newbury, M. Pepper, H. Ahmed, J. E. F. Frost, D. G. Hasko, D. C. Peacock, D. A. Ritchie, and G. A. C. Jones, J. Phys. C **21**, L209 (1988).
[8] E. A. Montie, E. C. Cosman, G. W. 't Hooft, M. B. Van der Mark, and C. W. J. Beenakker, Nature (London) **350**, 594 (1991).
[9] C. W. J. Beenakker and H. van Houten, Phys. Rev. Lett. **66**, 3056 (1991).
[10] H. Takayanagi, T. Akazaki, and J. Nitta, Phys. Rev. Lett. **75**, 3533 (1995).
[11] P. Debray, S. M. S. Rahman, J. Wan, R. S. Newrock, M. Cahay, A. T. Ngo, S. E. Ulloa, S. T. Herbert, M. Muhammad, and M. Johnson, Nat. Nanotechnol. **4**, 759 (2009).
[12] F. Meier and D. Loss, Phys. Rev. Lett. **90**, 167204 (2003).
[13] M. Meschke, W. Guichard, and J. P. Pekola, Nature (London) **444**, 187 (2006).
[14] T. Ojanen and T. T. Heikkilä, Phys. Rev. B **76**, 073414 (2007).
[15] O. Chiatti, J. T. Nicholls, Y. Y. Proskuryakov, N. Lumpkin, I. Farrer, and D. A. Ritchie, Phys. Rev. Lett. **97**, 056601 (2006).
[16] S. Jezouin, F. D. Parmentier, A. Anthore, U. Gennser, A. Cavanna, Y. Jin, and F. Pierre, Science **342**, 601 (2013).
[17] L. Cui, W. Jeong, S. Hur, M. Matt, J. C. Klöckner, F. Pauly, P. Nielaba, J. C. Cuevas, E. Meyhofer, and P. Reddy, Science **355**, 1192 (2017).
[18] L. G. C. Rego and G. Kirczenow, Phys. Rev. Lett. **81**, 232 (1998).
[19] M. P. Blencowe, Phys. Rev. B **59**, 4992 (1999).
[20] K. Schwab, E. A. Henriksen, J. M. Worlock, and M. L. Roukes, Nature (London) **404**, 974 (2000).

[21] Y. H. Xu, *Ferroelectric Materials and their Applications* (Elsevier, New York, 2013).
[22] N. A. Spaldin, Top. Appl. Phys. **105**, 175 (2007).
[23] Y. Kajiwara, K. Harii, S. Takahashi, J. Ohe, K. Uchida, M. Mizuguchi, H. Umezawa, H. Kawai, K. Ando, K. Takanashi, S. Maekawa, and E. Saitoh, Nature (London) **464**, 262 (2010).
[24] L. J. Cornelissen, K. J. H. Peters, G. E. W. Bauer, R. A. Duine, and B. J. van Wees, Phys. Rev. B **94**, 014412 (2016).
[25] K. Uchida, J. Xiao, H. Adachi, J.-i. Ohe, S. Takahashi, J. Ieda, T. Ota, Y. Kajiwara, H. Umezawa, H. Kawai, G. E. W Bauer, S. Maekawa, and E. Saitoh, Nat. Mater. **9**, 894 (2010).
[26] J. Flipse, F. K. Dejene, D. Wagenaar, G. E. W. Bauer, J. Ben Youssef, and B. J. Van Wees, Phys. Rev. Lett. **113**, 027601 (2014).
[27] S. Daimon, R. Iguchi, T. Hioki, E. Saitoh, and K. Uchida, Nat. Commun. **7**, 13754 (2016).
[28] G. E. W. Bauer, R. Iguchi, and K. Uchida, Phys. Rev. Lett. **126**, 187603 (2021).
[29] M. Büttiker, Phys. Rev. B **46**, 12485 (1992).
[30] S. Datta, *Electronic Transport in Mesoscopic Systems* (Cambridge University Press, Cambridge, England, 1997).
[31] Since ferron (magnon) reservoirs cannot be biased by electric (magnetic) fields for longer than their relaxation times, the field-driven currents are transient on this time-scale. We thank Bart van Wees for pointing out this oversight.
[32] M. Born and K. Huang, *Dynamical Theory of Crystal Lattices* (Clarendon Press, Oxford, 1954).
[33] J. D. Freire and R. S. Katiyar, Phys. Rev. B **37**, 2074 (1988).
[34] J. Pouget, A. Aşkar, and G. A. Maugin, Phys. Rev. B **33**, 6304 (1986).
[35] See Supplemental Material at http://link.aps.org/supplemental/10.1103/PhysRevLett.128.047601 for the derivation of the transport coefficients.
[36] Ph. Ghosez, E. Cockayne, U. V. Waghmare, and K. M. Rabe, Phys. Rev. B **60**, 836 (1999).
[37] J. Hlinka and P. Márton, Phys. Rev. B **74**, 104104 (2006).
[38] T. I. Andersen, B. L. Dwyer, J. D. Sanchez-Yamagishi, J. F. Rodriguez-Nieva, K. Agarwal, K. Watanabe, T. Taniguchi, E. A. Demler, P. Kim, H. Park, and M. D. Lukin, Science **364**, 154 (2019).
[39] D. M. Juraschek, M. Fechner, A. V. Balatsky, and N. A. Spaldin, Phys. Rev. Mater. **1**, 014401 (2017).
[40] K. Dunnett, J.-X. Zhu, N. A. Spaldin, V. Juričić, and A. V. Balatsky, Phys. Rev. Lett. **122**, 057208 (2019).
[41] R. M. Geilhufe, V. Juričić, S. Bonetti, J.-X. Zhu, and A. V. Balatsky, Phys. Rev. Research **3**, L022011 (2021).